Stephen J. Newsholme[1]
Beverly F. Maleeff[1]
Sandra Steiner[2]
N. Leigh Anderson[2]
Lester W. Schwartz[1]

[1]Safety Assessment, SmithKline Beecham Pharmaceuticals, King of Prussia, PA, USA
[2]Large Scale Proteomics Corporation, Rockville, MD, USA

Two-dimensional electrophoresis of liver proteins: Characterization of a drug-induced hepatomegaly in rats

Two-dimensional electrophoresis (2-DE) of liver proteins was applied to further characterize an unusual drug-induced increase in heptocellular rough endoplasmic reticulum (RER) in Sprague-Dawley rats given a substituted pyrimidine derivative. Absolute liver weights of drug-treated rats (9.9 ± 0.4 g) increased above vehicle-treated controls (7.2 ± 0.2 g) by 37%. Light microscopy revealed diffuse granular basophilia of the hepatocellular cytoplasm, uncharacteristic of hepatocytes and suggested cells rich in ribosomes, which was confirmed by electron microscopy. Immunostaining for cell proliferation, *viz*., 5-bromo-2'-deoxyuridine (BrdU) and proliferating cell nuclear antigen (PCNA), indicated marked hepatocellular proliferative activity. 2-DE of solubilized liver using an ISO-DALT gel system indicated significant (p<0.001) quantitative changes in at least 17 liver proteins (12 increased, 5 decreased) compared to controls. The protein with the largest increase was homologous to acute-phase reactant, contrapsin-like protein inhibitor-6. Other markedly upregulated proteins were methionine adenosyltransferase, a catalyst in methionine/ATP metabolism and mitochondrial HMG-CoA synthase, involved in cholesterol synthesis. The complementary strategies of 2-DE coupled either with database spot mapping or protein isolation and amino acid sequencing successfully identified a subset of proteins from xenobiotic-damaged rodent livers, the expression of which differed from controls. However, the current bioinformatics platform for rodent hepatic proteins and limited knowledge of specific protein functionality restricted application of this proteomics profile to further define a mechanistic basis for this unusual hepatotoxicity.

Keywords: Hepatomegaly / Rat liver / Two-dimensional polyacrylamide gel electrophoresis / Acute-phase reactants / Hepatocellular proliferation / Pyrimidine derivative EL 4016

1 Introduction

Two-dimensional electrophoresis (2-DE), a technique which enables resolution and quantification of hundreds of proteins simultaneously, has driven enthusiasm to completely define proteins expressed in diseased tissue. 2-DE, backed by recent advances in robotics, alternative protein screening methodologies and data mining of bioinformatics platforms, is beginning to offer opportunities to characterize complex patterns of tissue protein expression associated with the administration of xenobiotics or with spontaneous diseases. These protein pattern profiles may potentially represent signatures of specific host/organ responses or offer insights into pathogenic processes and/or potential surrogate markers for specific toxicity or disease process. A rudimentary database of rat liver proteins and 2-DE characterization of some xenobiotic responses has been initiated [1, 2]. Profiling the proteome of xenobiotic-damaged rodent livers has the long-term objectives of (i) assisting in investigations of molecular mechanisms of hepatotoxicity, and (ii) establishing signature patterns of liver toxicity for high-throughput screening of drug candidates.

During early preclinical assessment of drug candidates, we identified by histopathology an unusual hepatomegaly in rats treated with a series of substituted pyrimidine derivatives [3]. Light microscopy revealed enlarged hepatocytes with an unusual cytoplasmic basophilia, atypical of the usually eosinophilic hepatocyte cytoplasm; this appearance suggested liver cells rich in ribosomes. Ultrastructural assessment confirmed an abundance of membrane-bound ribosomes and arrays of vesiculated rough

Correspondence: Dr. Stephen J. Newsholme, SmithKline Beecham Pharmaceuticals, 709 Swedland Road, P.O. Box 1539, King of Prussia, PA 19406, USA
E-mail: stephen_j_newsholme@sbphrd.com
Fax: +610-270-7622

Abbreviations: BrdU, 5-bromo-2'-deoxyuridine; **H & E**, hematoxylin and eosin; **MS**, master spot; **PCNA**, proliferating cell nuclear antigen; **RER**, rough endoplasmic reticulum; **SER**, smooth endoplasmic reticulum

 0173-0835/00/1111-2122 $17.50+.50/0

endoplasmic reticulum (RER). Hepatomegaly is a well-recognized response of the rodent liver to xenobiotics and is generally associated either with an abundance of smooth endoplasmic reticulum (SER) and increased microsomal cytochrome P450 [4, 5], or with granular eosinophilic cytoplasm and peroxisome proliferation [6, 7]. Features of this pyrimidine-induced rodent hepatomegaly were clearly distinct from either of the typical rodent responses. Since cellular protein synthesis resides predominantly within RER, it was hypothesized that this unusual rodent hepatomegaly with abundant RER would be associated with an abundance of protein synthesis and perhaps with a specific protein, unique to this particular drug-induced event. Consequently, 2-DE was utilized to characterize the protein profile. Specifically, we sought to test the ability of 2-DE to (i) identify the principal protein products, (ii) to further define at a molecular level the mechanism of this hepatomegaly and (iii) to produce a protein signature pattern which would be of value to future drug candidate screening. Further, since liver enlargement was a prominent feature, the magnitude of hepatocellular proliferation was characterized using both exogenous and endogenous markers of cell proliferation.

2 Materials and methods

2.1 Animals

Female Sprague-Dawley (Crl:CD®BR) rats were obtained from Charles River Laboratories (Raleigh, NC). Following quarantine procedures, rats were acclimatized to local housing conditions for at least seven days and were 9–10 weeks old at study start. Rats were housed individually in stainless-steel cages in a controlled environment (68–76°F; 40–70% relative humidity) with 12 h light-dark cycle and were offered certified Rodent Diet #5002 (PMI Feeds, St. Louis, MO) and filtered tap water *ad libitum*. The studies were conducted under veterinary supervision and conformed to NRC Guidelines for animal use [8].

2.2 Experimental design

A substituted pyrimidine analog was administered to rats (10/group) once daily by oral gavage for seven days, as a suspension in 1% aqueous methyl cellulose (Sigma, St. Louis, MO); controls received an equivalent volume (10 mL/kg) of the vehicle only. To assess hepatocellular proliferative activity, an osmotic minipump (Alzet model 2ML1, 10 μL/h; Alza Corporation, Palo Alto, CA) was implanted subcutaneously, under isoflurane inhalation anesthesia (Florane; Ohio Medical Products, Madison, WI), into the back of each rat on the first day of study and 5-bromo-2'-deoxyuridine (BrdU; 20 mg/mL in 0.01 N NaOH; Sigma) was continuously delivered to each rat over the course of the 2-day experiment. Rats were killed by carbon dioxide exposure, the livers were weighed and slices collected from the left and right lateral lobes for microscopy. For 2-DE, approximately 0.5 g of liver tissue was taken from the apical end of the left liver lobe of each rat and held on ice prior to solubilization.

2.3 Light and electron microscopy

Liver slices were immersion-fixed in 10% neutral buffered formalin, routinely processed to 5 μm paraffin sections, stained with hematoxylin and eosin (H&E) and examined by light microscopy. For ultrastructural evaluation, portions, of formalin-fixed liver were transferred to phosphate-buffered 2.5% glutaraldehyde and processed into epoxy resin. Thin sections (70 nm) were collected on copper grids, stained with uranyl acetate and lead citrate and examined with a JEOL 1200EX transmission electron microscope.

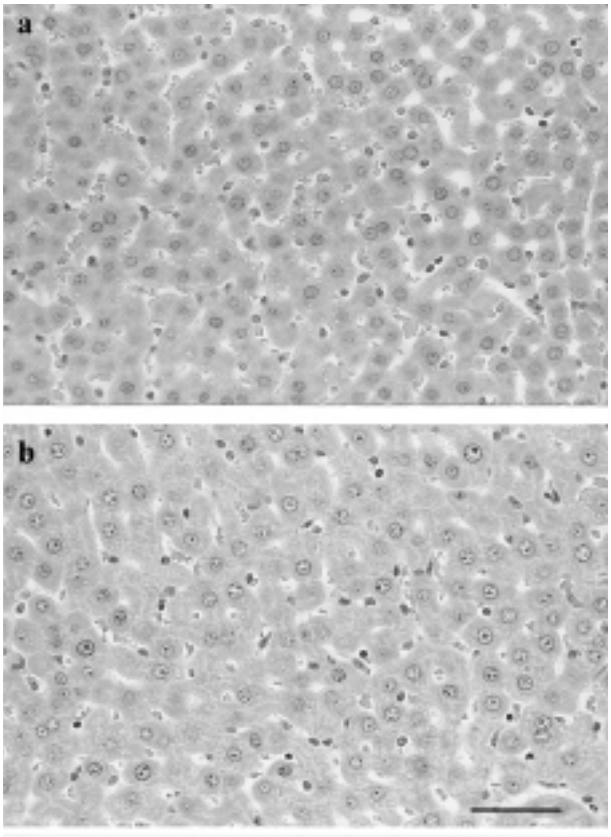

Figure 1. Photomicrographs of rat liver sections stained concurrently with hematoxylin and eosin from (a) a control and (b) a rat given pyrimidine derivative for 7 days. Hepalocytes of pyrimidine-treated rat are uniformly more blue than those of control, but cells do not differ in size. Bar = 50 μM.

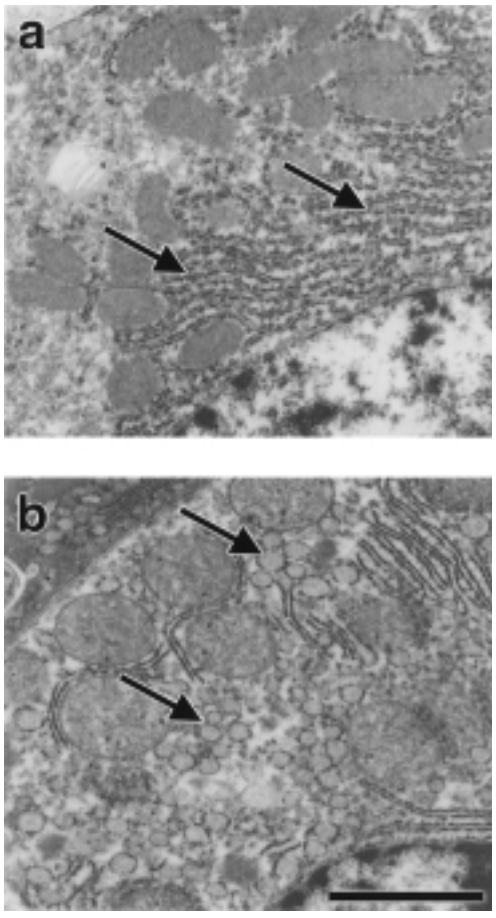

Figure 2. Transmission electron micrographs of portion of a hepatocyte from (a) a control and (b) a rat given pyrimidine derivative for 7 days. Heptocyte from drug-treated rat possesses abundant profiles of vesiculated RER (arrows) in contrast to the orderly RER profiles of the control. Bar = 1.5 μM.

2.4 Assessment of hepatocellular proliferation

The percentages of hepatocytes in S-phase (labeling index) from pyrimidine-treated and control rats were calculated from paraffin sections of liver stained immunohistochemically for BrdU incorporation [9] using a BrdU monoclonal antibody (Anti-BrdU; Becton Dickinson, San Jose, CA) and an anti-mouse IgG biotinylated secondary antibody (Vector Laboratories, Bulingame, CA), followed by streptavidin (Streptavidin-HRP; DAKO, Carpinteria, CA) and 3,3-diaminobenzidine staining. A labeling index was obtained by counting 1000 hepatocytes/rat. Additional sections were stained immunohistochemically for the endogenous replication marker, proliferating cell nuclear antigen (PCNA) [10, 11], using a PCNA monoclonal antibody (Coulter Corporation, Hialeah, FL) and an anti-mouse IgM biotinylated secondary antibody (Vector Laboratories) followed by streptavidin and 3,3-diaminobenzidine. A proliferating index was obtained based on 1000 hepatocytes/rat.

Table 1. Hepatocellular labeling indices for pyrimidine-treated rats and controls

	Hepatocellular labeling index (%; mean ± SEM)		
Antibody	Controls	Pyrimidine-treated	*p*-value[a)]
BrdU	13.48±1.98	48.37±4.39	0.00008
PCNA	19.59±4.97	37.72±5.49	0.02476

a) Comparison of mean by non-paired, 1-tailed *t*-test; $n = 10$

2.5 2-DE

Liver samples were homogenized in eight volumes of 9 M urea, 2% NP-40 detergent, 0.5% dithiothreitol (DTT) and 2% pH 8–10.5 Pharmalytes. The homogenates were centrifuged at 420 000 × *g* at 22°C for 30 min (TL 100 ultracentrifuge, TLA 100.3 rotor, 100 000 rpm; Beckman Instruments, Palo Alto, CA). The supernatant was removed, divided into four aliquots and stored at –80°C until analysis. Sample proteins were resolved by 2-DE using the 20 × 25 cm ISO-DALT 2-D gel system [12] operating with 20 gels per batch. All first-dimensional isoelectric focusing gels were prepared using the same single standardized batch of carrier ampholytes (BDH 4-8A) selected by Large Scale Biology's batch testing program for all rat and mouse database work. Eight μL of solubilized liver protein were applied to each gel, and the gels were run for 33 000–34 500 Vh using a progressively increasing voltage protocol implemented by a programmable high voltage power supply. An Angelique computer-controlled gradient casting system was used to prepare second-dimensional SDS gradient slab gels in which the top 5% of the gel was 11% T acrylamide, and the lower 95% varied linearly from 11% to 18% T. First-dimensional IEF tube gels were loaded directly onto the slab gels without equilibration and held in place by polyester fabric wedges (Wedgies) to avoid the use of hot agarose. Second-dimensional slab gels were run in groups of 20 in thermal-regulated (10°C) DALT tanks with buffer circulation. Following SDS electrophoresis, the slab gels were fixed overnight in 1.5 L/10 gels of 50% ethanol/3% phosphoric acid and then washed three times for 30 min in 1.5 L/10 gels of cold double ionized water. They were transferred to 1.5 L/10 gels of 34% methanol/17% ammonium sulfate/3% phosphoric acid for 1 h and after the addition of 1 g powdered Coomassie Brilliant Blue G-250 the gels were stained for three days to achieve equilibrium intensity. Stained slab gels were digitized in red light at 133 μm

resolution, using an Eikonix 1412 scanner and images were processed using the Kepler software system as described previously [13]. The liver master 2-D pattern used in this study was Wistarliv1. This master was used and described in previous studies [14]. A Student *t*-test was used to detect quantitative protein changes between control and treated groups with a cutoff made at $p < 0.001$. This yielded a total of 52 spots with significant abundance changes. Spots were identified from their master spot numbers in the Wistar rat liver master number database (MS numbers).

3 Results

3.1 Liver weight and morphology

The mean absolute liver weight of pyrimidine-treated rats increased above that of controls by 37% (9.9±0.4 g *vs.* 7.2 ± 0.2 g) and mean relative weight, based on body weight, increased 55% above control values. Light microscopic examination of H&E sections from pyrimidine-treated rats revealed cytoplasm of hepatocytes that was conspicuously more basophilic than in concurrently stained liver sections from controls (Fig. 1). This tinctorial change was present diffusely throughout the hepatic lobules. Hepatocytes from treated and controls rats appeared of similar size but occasional mitotic figures were observed within livers from pyrimidine-treated rats; inflammatory cell infiltrates and/or hepatocellular necrosis was not a feature of this drug-induced response. Bile ducts and the vasculature appeared normal. By electron microscopy, hepatocellular cytoplasm of pyrimidine-treated rats contained abundant membrane-bound ribosomes and arrays of vesiculated RER in contrast to orderly, non-vesiculated RER observed in controls (Fig. 2).

3.2 Assessment of hepatocellular proliferation

The hepatocellular labeling indices obtained from BrdU and from PCNA immunostaining are shown in Table 1. Both were significantly increased with drug treatment when compared to controls, indicating a hepatocellular proliferative effect of drug over the course of the study.

3.3 2-DE

There were significant ($p<0.001$) abundance changes in 52 spots of which 36 increased and 16 decreased (pyrimidine-treated rats *vs.* controls). One protein increased 12-

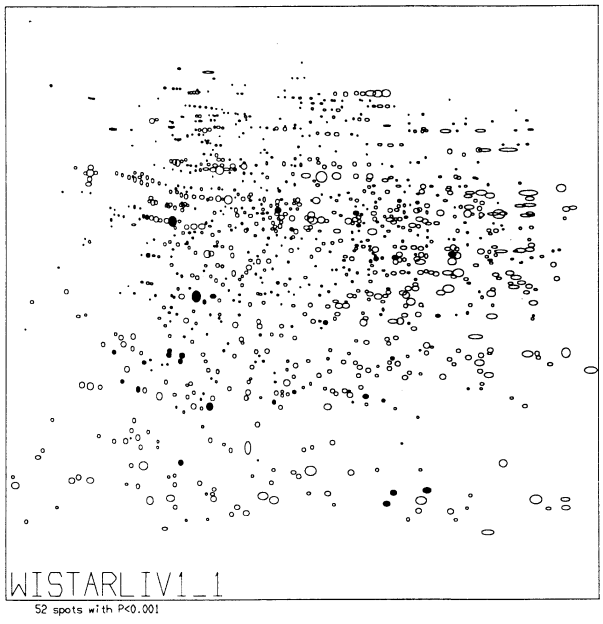

Figure 3. Map of protein spots showing the complete 2-D pattern with the 52 spots changes by treatment ($p < 0.001$) highlighted by filled ellipses and remaining spots shown as open ellipses. Molecular masses range from approximately 10–200 kDa (*y*-axis, bottom to top) and p*I* from 4 to 7 (*x*-axis, left to right).

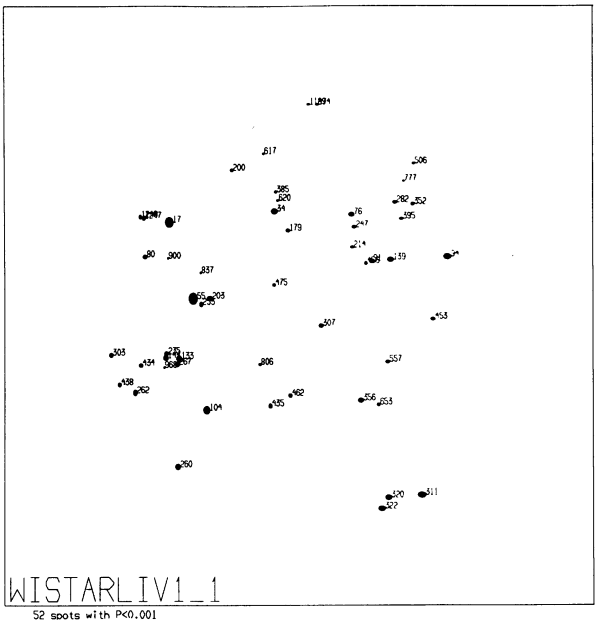

Figure 4. Map showing the 52 protein spots changed by treatment ($p < 0.001$) with their spot master numbers in the Wistar rat liver master number system. Molecular masses range from approximately 10 to 200 kDa (*y*-axis, bottom to top) and p*I* from 4 to 7 (*x*-axis, left to right).

fold and six other proteins increased 3 to 6-fold above control. Two schematic 2-D maps are presented (Figs. 3 and 4) showing the locations of these spots and their MS numbers. A series of bar graphs (Fig. 5) illustrates the normalized abundances of each protein on each gel.

3.4 Identity of proteins

From the 52 spots with significant abundance change with treatment, several proteins have been previously identified in the F344 rat liver reference 2-D pattern [1] which is linked to the Wistar rat liver reference 2-D pattern through a translation table. Seventeen proteins were identified from their MS number(s) and are listed in Table 2.

4 Discussion

The unusual morphological feature of this hepatomegaly was the abundance of RER within hepatocytes which, in this case, was coupled with a marked hepatocellular proliferative response. Replication of RER and associated accumulation of ribosomal ribose nucleic acid (rRNA) is an unusual drug-induced response in the rodent liver. In general, hepatomegaly in rodents is associated either with cytochrome P450 induction and SER replication or with peroxisomal proliferation. The morphological absence of SER corresponded with an assessment of hepatic cytochrome P450 enzyme activities in that an increase was not detected in these livers (data not shown). This was further correlated with the absence in abun-

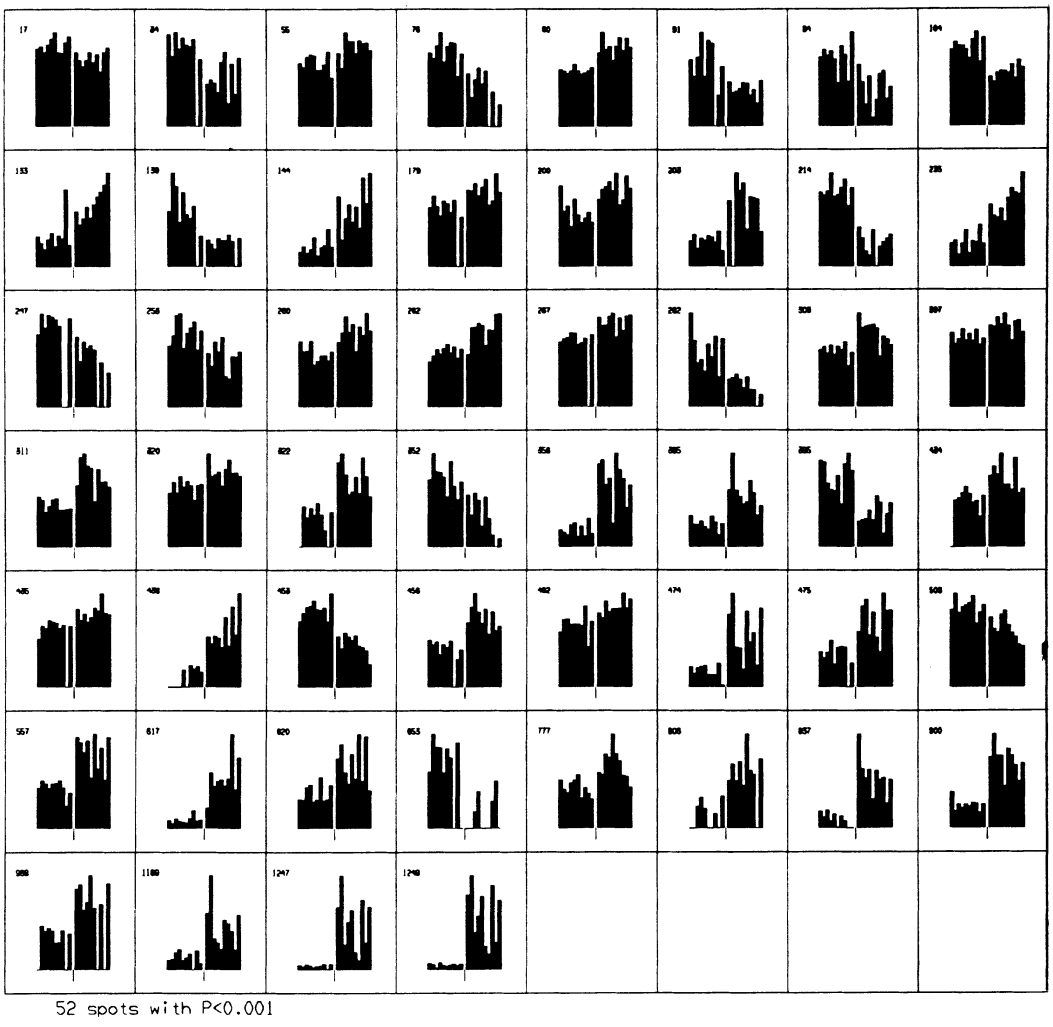

Figure 5. Bar graphs display normalized abundancies of each protein on each gel. Each panel represents the integrated Coomassie blue adsorbance measurements (abundance) for one protein, with MS number listed at top left of each panel. Each bar represents the value from one rat (controls on left, pyrimidine-treated on right).

Table 2. The 17 proteins, based on gel spots with significant ($p<0.001$) abundance change (pyrimidine treatment vs. control) identified from the Wistar-liv 1 MS numbers

MS Number	Abundance change *vs* control[a)]		Identity
55	↑	SMP30	Senescence marker protein 30
80	↑	LAMR	Laminin receptor
133,144,235	↑	HMGcoAS-f	Hydroxymethylglutaryl-coenzyme A synthase
307	↑	HO1	Heme oxygenase 1
320	↑	PKI1	Protein kinase C inhibitor 1
322	↑	DOPD_RAT	Dopachrome tautomerase
356	↑↑	ATPA_RAT	ATP synthase α-chain
385	↑	ER60_RAT	Probable protein disulfide isomerase ER-60
438	↑↑	PRCZ_RAT	Proteasome zeta-chain
474	↑↑	CPSM_RAT	Carbomyl-phosphate synthase (weak signal)
837	↑↑	METL_RAT	*S*-adenosylmethionine synthetase
1247,1249	↑↑↑		Contrapsin-like protein inhibitor 6
17	↓	ATPB	ATP synthase beta-chain
94	↓	ICDH	Isocitrate dehydrogenase
104	↓	MBP-23	23 kDa morphine-binding protein
139	↓	HPP_RAT	4-Hydroxyphenylpyruvate dioxygenase
395	↓	DHA5	Aldehyde dehydrogenase mitochondrial X precursor

a) increased <3-fold, ↑↑ 3 to 5-fold; ↑↑↑ 12-fold; ↓ decreased

dance changes for P450 proteins in the 2-DE assessment. Induction of hepatic cytochrome P450 was clearly not a feature of this hepatic response. Regarding peroxisomal proliferation, the morphological and 2-DE data also correlated: There was no ultrastructural evidence of increased hepatocellular peroxisomes nor of protein abundance increases of enzymes [15] associated with peroxisomal fatty acid β-oxidation.

Replication of RER, when observed in other cell types (*e.g.*, plasma cells), can be associated with increased serum concentrations of very homologous proteins, suggesting synthesis and secretion of consistent protein product. However, the serum protein concentrations in drug-treated rats from this study were comparable to control values; evidence of hyperproteinemia was not observed. Since numerous dilated vesicles were present within the hepatocellular RER, it appeared that the ribosomal product(s) were possibly being retained within hepatocytes. Based on histopathological experience with other hepatotoxicities, we did not attribute this striking degree of RER replication to the hepatocellular proliferative response, regardless of its magnitude. Accordingly, we hypothesized that this drug-induced replication of RER would be associated with a specific protein product and that 2-DE would allow isolation and identification. Unexpectedly, a complex array of 52 hepatocellular proteins, which were either increasing or decreasing in abundance, was identified.

The protein which increased to the greatest magnitude in the drug-treated rats was represented by two spots which closely resembled α_1-antitrypsin. Comparison of these spots (MS #1247 and 1249) to the Wistar rat liver master number database indicated homology to contrapsin-like protein inhibitor-6. Contrapsins are serine protease inhibitors synthesized in rat liver, they are acute-phase reactant and function in a variety of physiological and inflammatory processes. As markers of biological responses, contrapsins lack specificity and regulation of their expression is little understood. Kordula and co-workers [16] have studied three contrapsins from rat liver and provide data suggesting that interleukin-6 (IL-6), in conjunction with leukemia inhibitory factor (LIF) and glucocorticoids, functions to regulate contrapsin expression in primary cultures of rat hepatocytes. Since IL-6 has a regulatory role in hepatocellular proliferation [17], it is likely that the enhanced expression of contrapsin in these drug-treated rats was more reflective of the proliferative response rather than of the RER replication. An additional series of spots (MS #133, 144 and 235) was identified, again from the Wistar rat liver database, to represent mitochondrial hydroxymethylglutaryl-coenzyme A synthase (HMG-CoAS-f), an enzyme important in cholesterol synthesis. Clinical chemistry parameters (data not shown) monitored in rats given this substituted pyrimidine derivative for up to 1 month did not indicate altered cholesterol plasma concentrations as a consequence of enhanced HMG-CoAS-fi in these livers; consequently the biological implications of the increased intracellular enzyme concentrations are unknown. Enhanced expression of *S*-adenosylmethionine synthetase (MS#837) was also observed. This enzyme which catalyzes the formation of *S*-adenosylmethionine from methionine and ATP has been associated with rat hepatocellular regeneration [18].

The biological implication of alterations in abundance of other proteins in this rat liver response, including those which decreased in abundance with treatment (ATP synthase β-chain, isocitrate dehydrogenase, 23 kDa morphine-binding protein, and 4-hydroxyphenylpyruvate deoxygenase) are even less clear. Of the 36 spots which

increased in abundance, including two (MS #617 and 1189) which increased more than 3-fold, and also of the 16 spots which decreased in abundance, the majority remain to be identified. Until platform databases of protein identity are more complete and accessible to investigators, and details of protein expression, regulation and protein functionality are better defined, the interpretation of these complex protein profiles in context of their mechanistic implication in diseased organs will necessarily remain restricted.

In summary, application of 2-DE to characterize the proteome of rat hepatocytes which displayed a unusual hepatomegaly resulted in a successful characterization of a complex array of altered liver proteins. Consistent with challenges becoming more broadly recognized in the science of proteomics [19], the current limited state of knowledge regarding liver protein identities, function, pathway interactions and ultimate biological outcomes constrained our intepretative ability; this protein data set provided little to further understanding of the mechanism(s) or pathological consequences of this liver response. Considerable challenges remain ahead in the definition of protein signatures and in the functional characterization of a broad assortment of proteins.

The authors thank Ms Kate Rhodes for technical assistance with assessment of hepatocellular proliferation.

Received January 14, 2000

5 References

[1] Anderson, N. L., Esquer-Blasco, R., Hofmann, J.-P., Meyhaus, L., Raymackers, J., Steiner, S., Witzmann, F., Anderson, N. G., *Electrophoresis* 1995, *16*, 1977–1981.

[2] Anderson, N. L., Taylor, J., Hofmann, J.-P., Esquer-Blasco, R., Swift, S., Anderson, N. G., *Toxicol. Pathol.* 1996, *24*, 72–76.

[3] Newsholme, S. J., Maleeff, B. E., Anderson, N. L., Schwartz, L., *Toxicol. Sci.* 1998, *42*, 368.

[4] Schulte-Hermann, R., *CRC Crit. Rev. Toxicol.* 1974, *33*, 97–1974.

[5] Massey, E. D., Butler, W. H., *Chem. Biol. Interact.* 1978, *24*, 329–344.

[6] Reddy, J. K., Lalwini, N. D., *CRC Crit. Rev. Toxicol.* 1983, *12*, 1–58.

[7] Reddy, J. K., Warren, J. R., Reddy, M. K., Lalwini, N. D., *Ann. N. Y. Acad. Sci.* 1982, *386*, 81–110.

[8] National Research Council, *Guide for the Care and Use of Laboratory Animals*, National Academy Press, Washington, DC 1996.

[9] Eldridge, S. R., Tilbury, L. F., Goldsworthy, T. L., Butterworth, E. B., *Carcinogenesis* 1990, *11*, 2245–2251.

[10] Foley, J. F., Ton, T., Maronpot, R. R., Butterworth, B., Goldworthy, T. L., *Environ Health Perspect.* 1993, *101*, 199–206.

[11] Eldridge, S. R., Butterworth, B. E., Goldworthy, T. L., *Environ. Health Perspect.* 1993, *101*, 211–218.

[12] Anderson, N. L., *Two-Dimensional Electrophoresis Operation of the ISO-DALT System*, Large Scale Biology Press Washington, DC 1998, pp. 1–170.

[13] Anderson, N. L., Esquer-Blasco, R., Hofmann, J.-P., Anderson, N. G., *Electrophoresis* 1991, *12*, 907–930.

[14] Arce, A., Aicher, L., Wahl, D., Anderson, N. L., Meheus, L., Raymackers, J., Cordier, A., Steiner, S., *Life Sci.* 11998, *63*, 2243–2250.

[15] Parker, G. L., Orton, T. C., in: Gustafsson, J. A., Carlstedt-Duke, J., Mode, A., Rafter, J. (Eds.), *Biochemistry, Biophysics and Regulation of Cytochrome P-450*, Elsevier/North Holland Biomedical Press, Amsterdam 1980, p. 373.

[16] Kordula, T., Bugno, M., Lason, W., Przewlocki, R., Koj, A., *Biochem. Biophys. Res. Commun.* 1994, *201*, 222–227.

[17] Scotte, M., Masson, S., Lyoumi, S., Hiron, M., Teniere, P., Lebreton, J. P., Daveau, M., *Cytokine* 1997, *9*, 859–867.

[18] Frago, L. M., Giminez, A., Rodriquez, E. N., Varela-Nieto, I., *FEBS Lett.* 1998, *426*, 305–308.

[19] Abbott, A., *Nature* 1999, *402*, 715–720.